Available online at www.sciencedirect.com
SCIENCE DIRECT
Journal of Sound and Vibration 297 (2006) 315–328
JOURNAL OF SOUND AND VIBRATION
www.elsevier.com/locate/jsvi

The effects of kinematic model approximations on natural frequencies and modal damping of laminated composite plates

M. Soula[a,*], R. Nasri[b], A. Ghazel[a], Y. Chevalier[c]

[a]*Unité De Recherche Génie des Matériaux, Département de Génie Mécanique, Ecole Nationale d'Ingénieurs de Tunis, B.P. 37 Le Belvedére 1002 Tunis, Tunisia*
[b]*Laboratoire des Systémes et de Mécanique Appliquée, Ecole Polytechnique de Tunisie, Tunisia*
[c]*LISMMA, Institut Supérieur de Mécanique de Paris, 3 rue Fernand Hainaut 93407 St Ouen cedex, France*

Received 15 September 2004; received in revised form 27 March 2006; accepted 5 April 2006
Available online 16 June 2006

Abstract

The present work deals with the effects of kinematics on the natural frequencies and modal damping of laminated composite plates. Three theories are considered, the classical laminated plate theory (CLPT), the first-order shear deformation theory (FSDT) and the third-order shear deformation theory (TSDT). The displacement field corresponding to a simply supported square laminated composite plate is introduced in the energy equation. The governing equations are then formulated for the laminated composite plates using the Hamiltonian principle. Equations of motion are established and then the harmonic free vibrations are studied. The complex frequencies are obtained from the characteristic equation, which gives the natural frequencies and the modal damping for each (m,n) mode. The effects of stacking sequence, rotary inertia and thickness to side ratio (h/a) on the natural frequencies and modal damping ratios are analyzed. The results lead to conclusions about the applicability of each of the plate theories CLPT, FSDT and HSDT.

1. Introduction

Natural frequencies and modal damping are important parameters for the dynamic analysis of structures. A large amount of analytical and experimental research has concentrated on the evaluation of dynamic properties of viscoelastically reinforced composite materials as used in laminated plates [1–7]. A review of the literature shows that the dynamic properties of composite laminated plates depend on many parameters such as displacement field, rotary inertia, stacking sequence and thickness to side ratio, etc. In predicting the behavior of laminated plates, many theories have been developed as discussed below. The classical laminated plate theory (CLPT) was developed by Cauchy, Poisson and Kirchhoff. The basic assumption of this theory is that the normal to the midplane before deformation remains straight and normal to the plane after deformation. This assumption implies that the transverse shear deformation in the thickness direction of the plate is ignored. Based on the CLPT, Leung and Zhou [8] studied the vibration and stability problem of

*Corresponding author. Fax: +216 71 87 39 48.
E-mail address: Soulamed2003@Yahoo.fr (M. Soula).

0022-460X/$ - see front matter © 2006 Elsevier Ltd. All rights reserved.
doi:10.1016/j.jsv.2006.04.002

composite laminated plates by using the dynamic stiffness matrix method. Ohta et al. [9] presented the damping analysis of fiber-reinforced plastic laminated composite plates. The maximum strain and kinetic energies of a cross-ply laminated plate were evaluated analytically based on the 3D theory of elasticity. Reddy and Kuppusamy [10] developed a finite-element scheme based on 3D elasticity. However, as the authors pointed out, the computational expense precludes the use of such 3D elements in problems that require a large number of elements. Huang and Dasgupta [11] proposed a semi-analytical 3D layerwise theory to solve various orders of natural frequencies and mode shapes of thick arbitrarily laminated composite cylindrical panels.

These studies showed that the CLPT yields inaccurate results for laminated thick plates and overestimates natural frequencies because of the assumption that the transverse shear stiffness of plates is infinite.

Lin et al. [12] and Alam and Asnani [13] later proposed the first-order transverse shear deformation theory (FSDT), which is based on the Mindlin–Reissner plate theory. The basic assumption of this theory is that the normal to the midplane before deformation remains straight but not normal to the midplane after deformation. FSDT takes into account the transverse shear deformation in the thickness direction of the plate. Using FSDT, Wang et al. [14] developed a meshless approach based on reproducing the kernel particle method for the flexural, free vibration and buckling analysis of laminated composite plates. Bert and Chen [15] and Reddy [16] developed closed-form and finite-element solutions for the free vibration of simply supported antisymmetric angle-ply laminated plates. However, FSDT was found reliable only for predicting low-frequency behavior of moderately thick composite laminated plates; see Ref. [17].

Reddy [10] proposed a third-order shear deformation theory (TSDT) using a displacement field with cubic variations with respect to the thickness direction, which yields a parabolic transverse shear stress distribution. TSDT was used by Khdeir [18] for free vibration analysis of crossply laminated plates. Koo [19] studied the effects of layerwise in-plane displacements on the fundamental frequencies and the specific damping capacity of composite laminated plates. Zhou et al. [20] analyzed the free vibration of thick isotropic and laminated composite rectangular plates, with point supports, using the finite layer method. Meunier and Shenoi [21] have developed an analytical method based on Reddy's refined high-order shear deformation theory to determine the natural frequencies and modal damping of specific fiber-reinforced plastic sandwich plates. Ostachowicz et al. [22] studied the influence of shape memory alloy (SMA) fibers on changes in natural frequencies and thermal buckling of a composite laminated plate with SMA. An analytical method introduced by Hufenbach et al. [23] has a clear advantage in the design of composite laminated cylindrical shells. Qian et al. [24] presented a method for identifying elastic and damping properties of composite laminates from vibration test data. The analysis model is established based on a finite-element model that accounts for the effects of transverse shear deformation and hysteretic damping. Yarlagadda and Lesieutre [25] have developed analytical method using a higher-order shear laminate theory and the Rayleigh–Ritz method to determine the effects of changes in ply orientation, temperature and thickness of the laminate on natural frequencies and damping of flexural vibration of continuous fiber-reinforced composite panels. Using a finite-element idealization, Pervez and Zabaras [26] presented the linear transient dynamic and damping analysis of laminated anisotropic composite plates. The obtained experimental results for unidirectional composite beams are used to predict the damping capacity of the studied plates. Makhecha et al. [27], using a formulation based on the finite-element procedure, have studied the effects of higher-order theory, that accounts for the realistic variation of the in-plane and transverse displacements through the thickness, on the modal damping and natural frequencies of thick composite laminated sandwich plates.

This paper presents an analytical method using CLPT, FSDT and TSDT theories to analyze the natural frequencies and modal damping of square laminated composite plates. The effects of displacement fields, rotary inertia, stacking sequence and thickness to side ratio (h/a) are studied. For each displacement field (CLPT, FSDT and TSDT) the Hamiltonian principle is used to derive the governing equations. Theses equations are applied to the simply supported (on all edges) square laminated composite plate in order to compute the complex natural frequencies. Finally, the validity of the assumption of deformations and the applicability of the plate theories CLPT, FSDT and TSDT are discussed.

2. Analytical equations

Consider a simply supported laminated composite square plate of total thickness h, side a and N layers. In the present analysis, the origin of the orthonormal coordinate system (x, y, z) is chosen at the mid-surface of the laminated plate as shown in Fig. 1. The displacements of the plate in the x, y and z directions are denoted by u, v and w, respectively.

2.1. Displacements fields of the three used theories

2.1.1. CLPT

This theory is based on the Cauchy, Poisson and Kirchhoff assumptions which maintain that the normal to the midplane before deformation remains normal after deformation. Then the displacement field in the (x, y, z) reference frame has the following form:

$$\mathbf{U}(M) = \begin{Bmatrix} u(x,y,z,t) \\ v(x,y,z,t) \\ w(x,y,z,t) \end{Bmatrix} = \begin{Bmatrix} u_0(x,y,t) - z\dfrac{\partial w_0}{\partial x} \\ v_0(x,y,t) - z\dfrac{\partial w_0}{\partial y} \\ w_0(x,y,t) \end{Bmatrix}, \tag{1}$$

where $M(x, y, z)$ is a point of the laminated plate, the plane $(x, y, z = 0)$ coincides with the mid-surface of the laminated plate and the z direction is the out of plane coordinate normal to the mid-surface. The displacements (u_0, v_0, w_0) are those of a point on the midplane.

2.1.2. FSDT

The FSDT is based on the Mindlin–Reissner plate theory where the transverse normal to the mid-surface does not remain so after deformation. This introduces transverse shear stress. The field displacement in the (x, y, z) coordinate system is given by

$$\mathbf{U}(M) = \begin{Bmatrix} u(x,y,z,t) \\ v(x,y,z,t) \\ w(x,y,z,t) \end{Bmatrix} = \begin{Bmatrix} u_0(x,y,t) + z\phi_x(x,y,t) \\ v_0(x,y,t) + z\phi_y(x,y,t) \\ w_0(x,y,t) \end{Bmatrix}, \tag{2}$$

where $M(x, y, z)$ and (u_0, v_0, w_0) are as defined above and ϕ_x and ϕ_y are rotations around the x- and y-axis, respectively.

2.1.3. TSDT

Based on the same assumptions as the CLPT and FSDT, Reddy [1,10] proposed the TSDT theory using a displacement field with cubic variations in the coordinate along the thickness direction. This yields a parabolic transverse shear stress distribution across each layer. The displacement field, in the (x, y, z) coordinate frame is

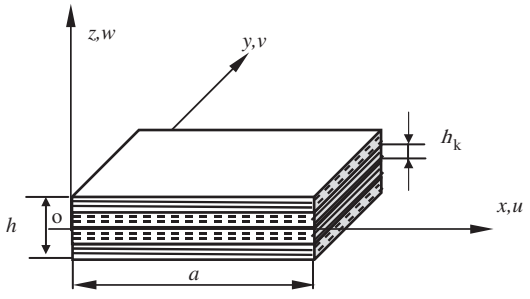

Fig. 1. Geometry and coordinates system of a multilayer composite plate.

given by

$$\mathbf{U}(M)=\begin{Bmatrix} u(x,y,z,t)\\ v(x,y,z,t)\\ w(x,y,z,t)\end{Bmatrix}=\begin{Bmatrix} u_0(x,y,t)+z\phi_x(x,y,t)-z^3c_1\left(\phi_x+\dfrac{\partial w_0}{\partial x}\right)\\ v_0(x,y,t)+z\phi_y(x,y,t)-z^3c_1\left(\phi_y+\dfrac{\partial w_0}{\partial y}\right)\\ w_0(x,y,t)\end{Bmatrix}, \tag{3}$$

where $c_1=(4/3h^2)$ and $M(x,y,z)$, (u_0,v_0,w_0), ϕ_x and ϕ_y are as defined above.

2.2. Laminate constitutive equations

2.2.1. Stress strain relation in the kth layer

The elastic isothermal stress–strain relations of the kth orthotropic layer of the composite laminate as shown in Fig. 2, are given in the local $(1,2,3)$ cartesian coordinate system by

$$\begin{Bmatrix}\sigma_1\\ \sigma_2\\ \sigma_4\\ \sigma_5\\ \sigma_6\end{Bmatrix}^{(k)}=\begin{bmatrix} Q_{11} & Q_{12} & 0 & 0 & 0\\ Q_{12} & Q_{22} & 0 & 0 & 0\\ 0 & 0 & Q_{44} & 0 & 0\\ 0 & 0 & 0 & Q_{55} & 0\\ 0 & 0 & 0 & 0 & Q_{66}\end{bmatrix}^{(k)}\begin{Bmatrix}\varepsilon_1\\ \varepsilon_2\\ \varepsilon_4\\ \varepsilon_5\\ \varepsilon_6\end{Bmatrix}, \tag{4}$$

where Q_{ij} are the elastic coefficients calculated using Young's modulus, shear modulus and Poisson's ratios of the laminate composite plate, defined by

$$Q_{11}=\frac{E_1}{(1-v_{12}v_{21})},\quad Q_{22}=\frac{E_2}{(1-v_{12}v_{21})},\quad Q_{12}=\frac{v_{12}E_2}{(1-v_{12}v_{21})}, \tag{5}$$

$$Q_{44}=G_{23},\quad Q_{55}=G_{13},\quad Q_{66}=G_{12}. \tag{6}$$

For orthotropic configurations the Q_{16}, Q_{26} and Q_{45} terms vanish. For a lamina of plates with ply angle θ, the transformed elastic constants $\bar{Q}_{ij}$ expressions are given in Appendix A.

2.2.2. Behavior laws of the laminate plate

The constitutive equations that relate the force and moment resultants to the laminate stresses are given by

$$\begin{Bmatrix}N_{\alpha\beta}\\ M_{\alpha\beta}\\ P_{\alpha\beta}\end{Bmatrix}=\int_{-h/2}^{h/2}\sigma_{\alpha\beta}\begin{Bmatrix}1\\ z\\ z^3\end{Bmatrix}\mathrm{d}z, \tag{7}$$

$$\begin{Bmatrix}Q_{\alpha}\\ R_{\alpha}\end{Bmatrix}=\int_{-h/2}^{h/2}\sigma_{\alpha z}\begin{Bmatrix}1\\ z^2\end{Bmatrix}\mathrm{d}z, \tag{8}$$

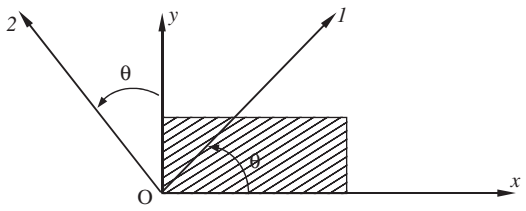

Fig. 2. Fiber orientation of the kth orthotropic layer.

where the subscripts α and β take on the values x and y, (N_{xx}, N_{yy}, N_{xy}) and (Q_x, Q_y) are components of the resultants forces $N_{\alpha\beta}$ and Q_α, respectively. (M_{xx}, M_{yy}, M_{xy}) are components of the resultants moments $M_{\alpha\beta}$, (P_{xx}, P_{yy}, P_{xy}) and (R_x, R_y) denote the higher-order stress resultants, which are relevant only for TSDT.

The constitutive equations of a laminate that relate the force and moment resultants **N**, **P** and **M** to the strains ($\boldsymbol{\varepsilon}^{(0)}$, $\boldsymbol{\varepsilon}^{(1)}$ and $\boldsymbol{\varepsilon}^{(3)}$) are deduced from the equations in appendix B as follows.

$$\begin{Bmatrix} \mathbf{N} \\ \mathbf{M} \\ \mathbf{P} \end{Bmatrix} = \begin{bmatrix} \mathbf{A} & \mathbf{B} & \mathbf{E} \\ \mathbf{B} & \mathbf{D} & \mathbf{F} \\ \mathbf{E} & \mathbf{F} & \mathbf{H} \end{bmatrix} \begin{Bmatrix} \boldsymbol{\varepsilon}^{(0)} \\ \boldsymbol{\varepsilon}^{(1)} \\ \boldsymbol{\varepsilon}^{(3)} \end{Bmatrix} \tag{9}$$

and

$$\begin{Bmatrix} \mathbf{Q} \\ \mathbf{R} \end{Bmatrix} = \begin{bmatrix} \mathbf{A} & \mathbf{D} \\ \mathbf{D} & \mathbf{F} \end{bmatrix} \begin{Bmatrix} \boldsymbol{\gamma}^{(0)} \\ \boldsymbol{\gamma}^{(2)} \end{Bmatrix}, \tag{10}$$

where the coefficients of the 3×3 and symmetric matrices **A**, **B**, **D**, **E**, **F**, and **H** of the laminate are defined by

$$\begin{Bmatrix} A_{ij} \\ B_{ij} \\ D_{ij} \\ E_{ij} \\ F_{ij} \\ H_{ij} \end{Bmatrix} = \sum_{k=1}^{N} \int_{z_k}^{z_{k+1}} \bar{Q}_{ij}^{(k)} \begin{Bmatrix} 1 \\ z \\ z^2 \\ z^3 \\ z^4 \\ z^6 \end{Bmatrix} \mathrm{d}z \tag{11}$$

k is the layer number and the $\bar{Q}_{ij}$ are defined in Appendix A.

For symmetric composite plates, the coupling stiffness matrix terms B_{ij} as well as higher-order terms E_{ij} are reduced to zero. The Q_{44} and Q_{55} terms characterize the shear distribution over the composite thickness in the 23 and 13 planes, respectively.

2.2.3. Equations of motion

The evaluation of the natural frequencies of the composite laminate plate is based on the Hamiltonian principle. The displacements (u_0, v_0, w_0) of a point on the midplane are introduced to satisfy the boundary conditions given in Appendix C. The resulting equations of motion can be written in a matrix form in terms of the generalized displacement vector **X** as

$$\mathbf{M}\ddot{\mathbf{X}} + \mathbf{K}^*\mathbf{X} = \mathbf{0}, \tag{12}$$

where **M** is the mass matrix, $\mathbf{K}^*$ is the complex stiffness matrix and $\mathbf{X}^{\mathrm{T}} = \{u_{mn}, v_{mn}, w_{mn}, X_{mn}, Y_{mn}\}$ as defined in Appendix C.

The study of harmonic free vibrations leads to solve the characteristic equation

$$|\mathbf{K}^* - \omega^2\mathbf{M}| = 0. \tag{13}$$

The complex natural frequency solutions $\omega^*(m,n)$ of Eq. (13) are given by

$$(\omega^*(m,n))^2 = p(m,n) + jq(m,n) = p(m,n)(1 + j\eta(m,n)), \tag{14}$$

where the (m,n) modal damping $\eta(m,n)$ is given by

$$\eta(m,n) = p(m,n)/q(m,n) \tag{15}$$

and the real natural frequency $\omega(m,n)$ is given by

$$\omega(m,n) = \sqrt{p(m,n)}. \tag{16}$$

For simplicity, the frequencies are expressed in the non-dimensional form

$$\varpi(m,n) = \omega(m,n)((a^2/h)\sqrt{\rho/E_2}). \tag{17}$$

3. Numerical results and analysis

In this section the dynamic behavior of a simply supported cross ply graphite epoxy laminated square plates is investigated. The effects of the kinematics, rotary inertia, stacking sequence and thickness to side ratio (h/a) on the natural frequencies and modal damping ratios are studied.

The stacking sequence is expressed by using the notation $[\theta1/\theta2/\theta3/\theta4/\ldots]$. For example $[0/90/90/0]$ denote a four-layered symmetric plate which has fiber angles $0^\circ, 90^\circ, 90^\circ$ and 0° successively from lower to upper layers in the plate.

The mechanical properties of the graphite epoxy are given by $E_1/E_2 = 20$, $G_{12}/E_2 = 0.65$, $G_{13} = G_{12}$, $G_{23}/E_2 = 0.5$, $v_{12} = 0.25$, $\eta_1 = 0.0015$, $\eta_2 = 0.01$ and $\eta_{12} = \eta_{13} = 0.016$ (Suffix 1 and 2 denote the kth fiber direction and the in-plane orthogonal direction, respectively as shown in Fig. 2).

3.1. Analysis of the effects of the rotary inertia (RI)

Figs. 3–6 show the effects of the rotary inertia on natural frequency and modal damping. Taking into account RI has an effect of decreasing the natural frequency especially at high-order mode. For the natural frequency, the difference between the cases with and without RI is within 3% for symmetric laminated plate and 4% for antisymmetric plate using CLPT. However, this difference is within 1.2% for symmetric plate and 1.4% for antisymmetric plate for the shear theories. These results are calculated for mode (4,4) and this difference increases with the mode order. For the CLPT, taking into account the RI has no effect on modal damping across all modes as shown in Figs. 3b–6b. Whereas, for shear theories a slight decrease in modal

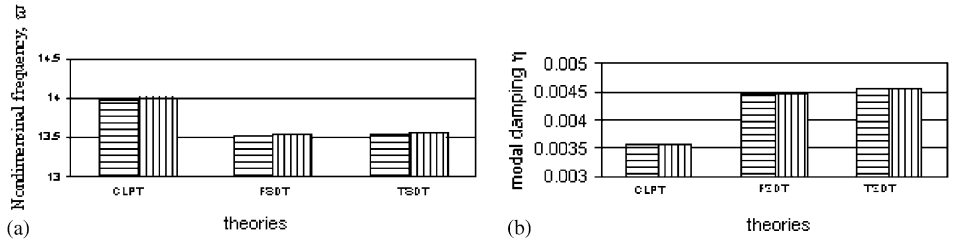

Fig. 3. (a) The effects of rotary inertia (RI) and displacement field on natural frequency at low mode $(1,1)$ for $h/a = 0.05$ and symmetric laminated plates $[0^\circ/90^\circ/90^\circ/0^\circ]$: ▤, with RI; ▥, without RI. (b) The effects of rotary inertia(RI) and displacement field on modal damping at low mode $(1,1)$ for $h/a = 0.05$ and symmetric laminated plates $[0^\circ/90^\circ/90^\circ/0^\circ]$: ▤, with RI; ▥, without RI.

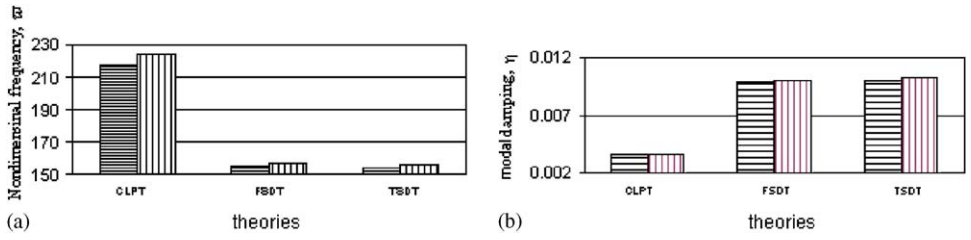

Fig. 4. (a) The effects of rotary inertia (RI) and displacement field on natural frequency at higher-order mode $(4,4)$ for $h/a = 0.05$ and symmetric laminated plates $[0^\circ/90^\circ/90^\circ/0^\circ]$: ▤, with RI; ▥, without RI. (b) The effects of rotary inertia (RI) and displacement field on modal damping at higher-order mode $(4,4)$ for $h/a = 0.05$ and symmetric laminated plates $[0^\circ/90^\circ/90^\circ/0^\circ]$: ▤, with RI; ▥, without RI.

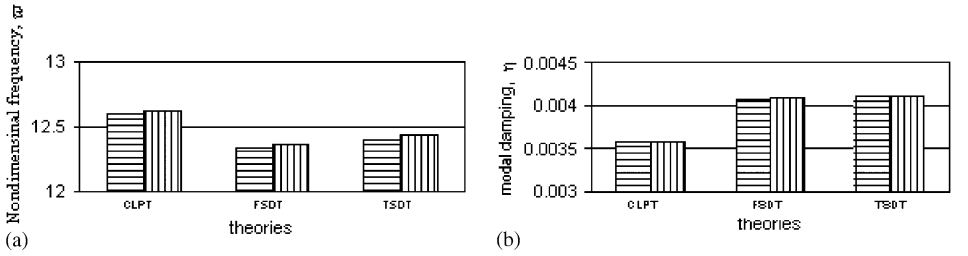

Fig. 5. (a) The effects of rotary inertia (RI) and displacement field on natural frequency at low mode $(1,1)$ for $h/a = 0.05$ and antisymmetric laminated plates $[0^\circ/90^\circ/0^\circ/90^\circ]$: ▤, with RI; ▥, without RI. (b) The effects of rotary inertia (RI) and displacement field on modal damping at low mode $(1,1)$ for $h/a = 0.05$ and antisymmetric laminated plates $[0^\circ/90^\circ/0^\circ/90^\circ]$: ▤, with RI; ▥, without RI.

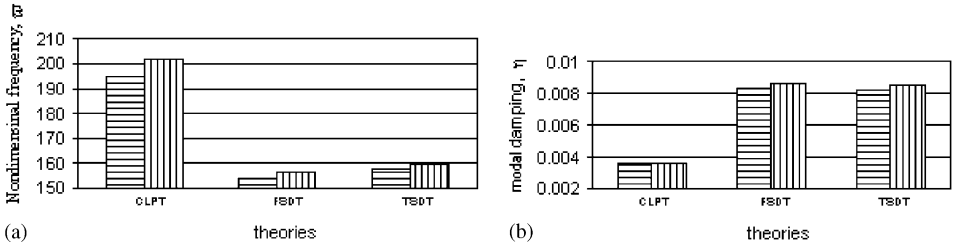

Fig. 6. (a) The effects of rotary inertia (RI) and displacement field on natural frequency at higher-order mode $(4,4)$ for $h/a = 0.05$ and antisymmetric laminated plates $[0^\circ/90^\circ/0^\circ/90^\circ]$: ▤, with RI; ▥, without RI. (b) The effects of rotary inertia (RI) and displacement field on modal damping at higher-order mode $(4,4)$ for $h/a = 0.05$ and antisymmetric laminated plates $[0^\circ/90^\circ/0^\circ/90^\circ]$: ▤, with RI; ▥, without RI.

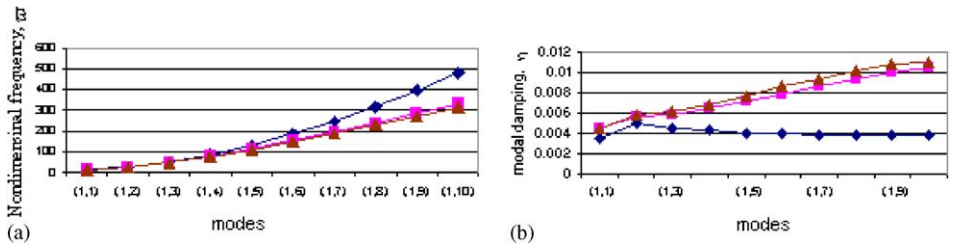

Fig. 7. (a) The effects of the displacement field and order of modes on natural frequency for symmetric laminated plate $[0^\circ/90^\circ/90^\circ/0^\circ]$, $h/a = 0.05$ and without rotary inertia (RI): ◆, CLPT; ■, FSDT; ▲, TSDT. (b) The effects of the displacement field and order of modes on modal damping for symmetric laminated plate $[0^\circ/90^\circ/90^\circ/0^\circ]$, $h/a = 0.05$ and without rotary inertia (RI): ◆, CLPT; ■, FSDT; ▲, TSDT.

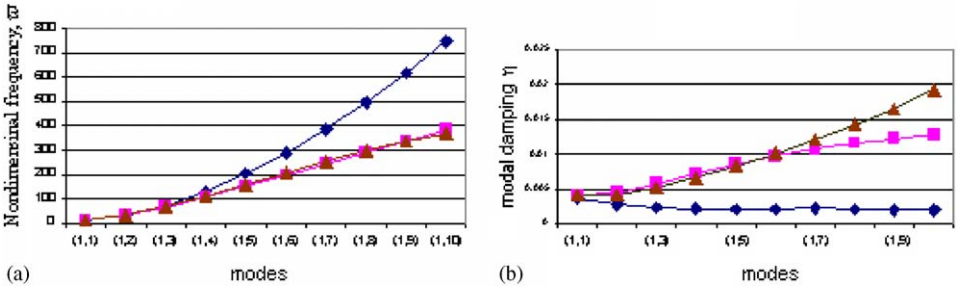

Fig. 8. (a) The effects of the displacement field and order of modes on natural frequency for antisymmetric laminated plate $[0^\circ/90^\circ/0^\circ/90^\circ]$ and $h/a = 0.05$ and without rotary inertia (RI): ◆, CLPT; ■, FSDT; ▲, TSDT. (b) The effects of the displacement field and order of modes on modal damping for antisymmetric laminated plate $[0^\circ/90^\circ/0^\circ/90^\circ]$ and $h/a = 0.05$ and without rotary inertia (RI): ◆, CLPT; ■, FSDT; ▲, TSDT.

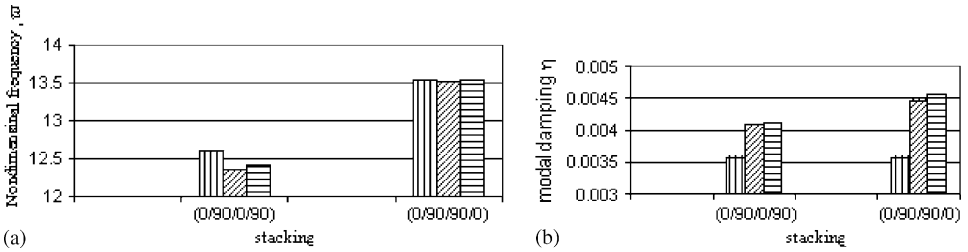

Fig. 9. (a) The effects of staking sequence and displacement field on natural frequency at low mode (1, 1) for $h/a = 0.05$ and without rotary inertia (RI): ▥, CLPT; ▨, FSDT; ▤, TSDT. (b) The effects of staking sequence and displacement field on modal damping at low mode (1, 1) for $h/a = 0.05$ and without rotary inertia (RI): ▥, CLPT; ▨, FSDT; ▤, TSDT.

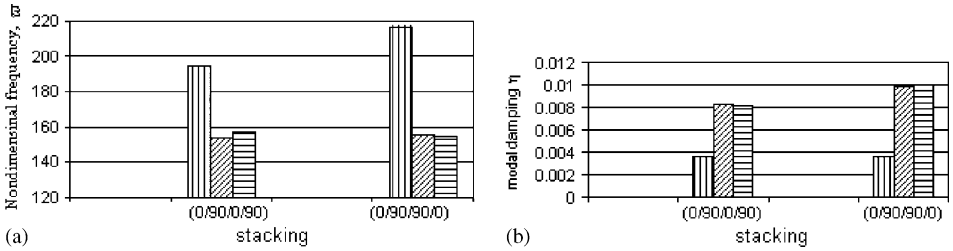

Fig. 10. (a) The effects of staking sequence and displacement field on natural frequency at higher-order mode (4, 4) for $h/a = 0.05$ and without rotary inertia (RI): ▥, CLPT; ▨, FSDT; ▤, TSDT. (b) The effects of staking sequence and displacement field on modal damping at higher-order mode (4, 4) for $h/a = 0.05$ and without rotary inertia (RI): ▥, CLPT; ▨, FSDT; ▤, TSDT.

damping is observed only for higher-order modes. This difference is within 3.4% for antisymmetric plate and 1.4% for symmetric plates. These results indicate that RI decreases natural frequency and modal damping at higher modes especially for shear theories and antisymmetric composite laminated plates (Figs. 7 and 8).

3.2. Analysis of the stacking sequence effects

Figs. 9a and 10a show that the natural frequencies are more important for the antisymmetric laminate plate [0/90/0/90] than for the symmetric laminate plate [0/90/90/0]. Figs. 9b and 10b show that the stacking sequence has no effect on the modal damping for CLPT. While, for FSDT and TSDT, the modal damping is higher, for the symmetric laminate plate, from 10% for mode (1, 1) to 20% for the (4, 4) mode. For a symmetric laminate plate, the effect of warping on the modal damping is small. However, for the antisymmetric laminate plate, warping increases the modal damping at higher-order modes.

The difference in natural frequency results obtained from the three theories (CLPT, CFDT, TSDT) for thin plates and at low modes are negligible for symmetric laminated plates as shown in Figs. 11 and 13. This is to be expected since there are no coupling effects (extension-flexure and extension-warping), i.e. ($B_{ij} = E_{ij} = 0$ for $i, j = 1, 2, 6$). In the case of antisymmetric laminated plates this difference is more pronounced. This is due to the coupling effects between extensional and flexural deformation expressed by the coefficients B_{ij} of the matrix **B** of Eq. (9) and the coupling effects between extensional and warping deformation expressed by the coefficients E_{ij} of the matrix **E** of Eq. (9). It should be noted that the difference in natural frequencies obtained from the three theories decrease as the number of layers increases (see Ref. [1]).

3.3. Analysis of the thickness ratio effects

Figs. 11–14 show that using the CLPT, the thickness to side ratio has a small effect on natural frequency. The difference between the results given for $h/a = 0.01-0.05$ is found to be less than 3%. The thickness to side

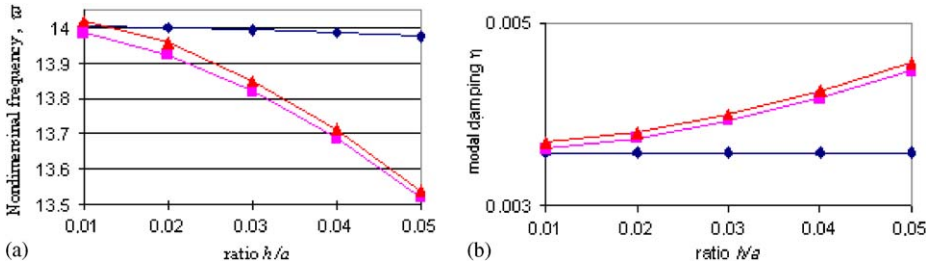

Fig. 11. (a) The effects of thickness to side ratio (h/a) and displacement field on natural frequency for symmetric laminated plate [0°/90°/90°/0°] and at low mode (1, 1), and without rotary inertia (RI): ◆, CLPT; ■, FSDT; ▲, TSDT. (b) The effects of thickness to side ratio (h/a) and displacement field on modal damping for symmetric laminated plate [0°/90°/90°/0°] and at low mode (1, 1) and without rotary inertia (RI): ◆, CLPT; ■, FSDT; ▲, TSDT.

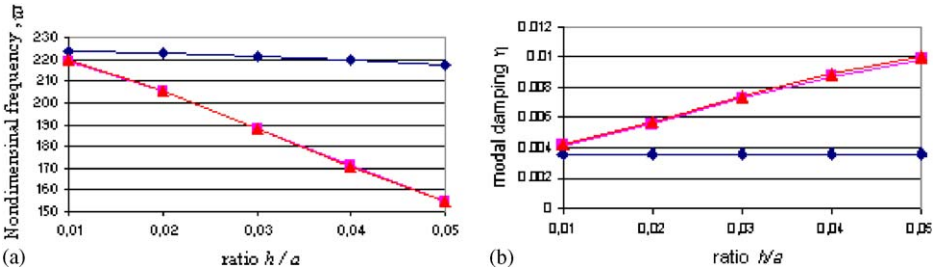

Fig. 12. (a) The effects of thickness to side ratio (h/a) and displacement field on natural frequency for symmetric laminated plate [0°/90°/90°/0°] at higher-order mode (4, 4), and without rotary inertia (RI): ◆, CLPT; ■, FSDT; ▲, TSDT. (b) The effects of thickness to side ratio (h/a) and displacement field on modal damping for symmetric laminated plate [0°/90°/90°/0°] at higher-order mode (4, 4) and without rotary inertia (RI): ◆, CLPT; ■, FSDT; ▲, TSDT.

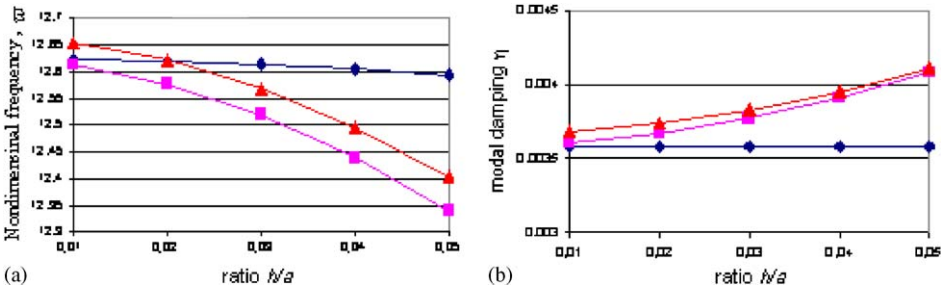

Fig. 13. (a) The effects of thickness to side ratio (h/a) and displacement field on natural frequency for antisymmetric laminated plate [0°/90°/0°/90°] at low mode (1, 1) and without rotary inertia (RI): ◆, CLPT; ■, FSDT; ▲, TSDT. (b) The effects of thickness to side ratio (h/a) and displacement field on modal damping for antisymmetric laminated plate [0°/90°/0°/90°] at low mode (1, 1) and without rotary inertia (RI): ◆, CLPT; ■, FSDT; ▲, TSDT.

ratio has no effect on modal damping. When using FSDT and TSDT, it is noted that an increase in thickness to side ratio leads to a decrease in the natural frequency and an increase in the modal damping. The reduction of the natural frequency results given for $h/a = 0.01-0.05$, are found to be less than 3% for lower modes (1.1) and they are within 30% for higher-order modes (4.4). However, the increase in modal damping for $h/a = 0.01-0.05$ are found to be, for lower modes (1.1), within 23% for symmetric laminated plates and within 13% for antisymmetric laminated plates.

For high modes (4.4), the modal damping results are within 137% for symmetric laminated plates and within 113% for antisymmetric laminated plates.

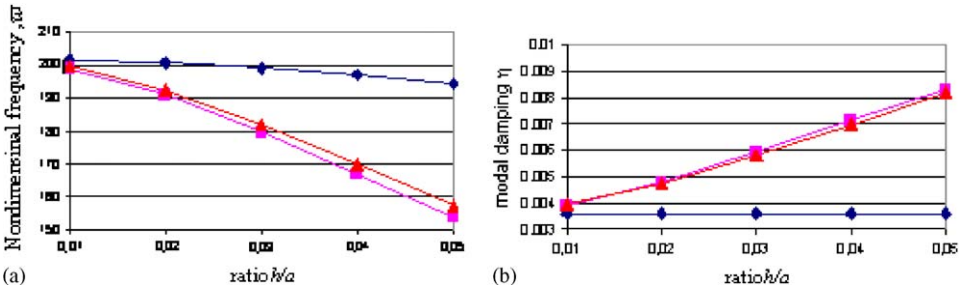

Fig. 14. (a) The effects of thickness to side ratio (h/a) and displacement field on natural frequency for antisymmetric laminated plate [0°/90°/0°/90°] at higher-order mode (4, 4) and without rotary inertia (RI): ◆, CLPT; ■, FSDT; ▲, TSDT. (b) The effects of thickness to side ratio (h/a) and displacement field on modal damping for antisymmetric laminated plate [0°/90°/0°/90°] at higher-order mode (4, 4) and without rotary inertia (RI): ◆, CLPT; ■, FSDT; ▲, TSDT.

3.4. Analysis of kinematic effects

In this section, results are found using a thickness side ratio $h/a = 0.05$ and rotary inertia effects are not considered.

Figs. 7 and 8 show that taking into account the shear strain decreases the natural frequency and increases the modal damping especially for higher-order modes and antisymmetric plates.

For symmetric plates, this difference in natural frequency is within 3% for mode (1,1) and 10% for mode (1, 10) and in modal damping, it is for the considered tow modes, within 25% and 176% respectively. However, for antisymmetric plates, the difference in natural frequency is within 2% for mode (1, 1) and 50% for mode (1, 10) and in modal damping, theses results became 14.3% and 568%, respectively.

Figs. 7b and 8b show that the modal damping obtained using CLPT is smaller that of FSDT or TSDT. The modal damping decreases with the mode order for CLPT while it increases for the FSDT and TSDT models.

If warping is taken into account, this will decrease natural frequency and increase modal damping especially for higher-order modes and antisymmetric plates. The difference, in natural frequency, is within 0.1% from the mode (1.1) to 3% for the (1.10) mode for symmetric plates, but these results become 2.3% and 2%, respectively for antisymmetric plates. For damping, the difference is within 3% for mode (1, 1) and 11% for mode (1, 10) for symmetric plates. However these results give 3% for mode (1, 1) and 360% for mode (1, 10) and antisymmetric plates. It is also seen that the shear strain has more influence than the warping.

4. Conclusion

The analytical methods presented in this paper allow the prediction of natural frequencies and modal damping of laminated composite symmetric and antisymmetric plates. Three plates theories CLPT, FSDT and TSDT are used. The effect of rotary inertia, stacking sequence, and thickness to side ratio (h/a) on the natural frequencies and modal damping ratios are studied for these displacement fields. It is found that the modal damping is higher for antisymmetric laminated plates than for symmetric laminated plates. These results was showed by Pervez and Zabaras [26] for an other material and by an other method. The natural frequencies are also higher for antisymmetric laminated plates than for symmetric laminated plates. These results depended on the number of layers of the laminate as indicated in Ref. [1].

The effect of rotary inertia increase with order of modes. This is more significant when the shear deformation is neglected. The CLPT overestimates natural frequencies and underestimate modal damping, this phenomena increases with the order of mode. Therefore, this theory can be used only at low-order modes. This means that shear deformation cannot be neglected with increasing mode order. The FSDT and TSDT predict higher modal damping and lower natural frequencies especially at higher-order modes. This phenomena is more noticeable with increasing thickness to side ratio (h/a) and especially for antisymmetric composite plates. It is also noted that FSDT and TSDT predict similar results for $h/a < 0.05$. However, for the thick plates, the warping must be considered especially for higher-order modes and especially for antisymmetric plates.

Acknowledgment

The authors gratefully acknowledge the reviewers, whose comment and remarks have contributed to the improvement of the final manuscript.

Appendix A

For a lamina of plates with ply angle θ Fig. 2, the transformed elastic constants $\bar{Q}_{ij}$ are given by

$$\begin{aligned}
\bar{Q}_{11} &= Q_{11}\cos^4\theta + Q_{22}\sin^4\theta + 2(Q_{12}+2Q_{66})\cos^2\theta\sin^2\theta,\\
\bar{Q}_{12} &= (Q_{11}+Q_{22}-4Q_{66})\cos^2\theta\sin^2\theta + Q_{12}(\cos^4\theta+\sin^4\theta),\\
\bar{Q}_{22} &= Q_{11}\sin^4\theta + Q_{22}\cos^4\theta + 2(Q_{12}+2Q_{66})\cos^2\theta\sin^2\theta,\\
\bar{Q}_{16} &= (Q_{11}-Q_{12}-2Q_{66})\cos^3\theta\,\sin\theta + (Q_{12}-Q_{22}+2Q_{66})\cos\theta\sin^3\theta,\\
\bar{Q}_{26} &= (Q_{11}-Q_{12}-2Q_{66})\cos\theta\sin^3\theta + (Q_{12}-Q_{22}+2Q_{66})\cos^3\theta\,\sin\theta,\\
\bar{Q}_{66} &= (Q_{11}+Q_{22}-2Q_{12}-2Q_{66})\cos^2\theta\sin^2\theta + Q_{66}(\cos^4\theta+\sin^4\theta),\\
\bar{Q}_{44} &= Q_{44}\cos^2\theta + Q_{55}\sin^2\theta,\\
\bar{Q}_{45} &= (Q_{55}-Q_{44})\cos\theta\sin\theta,\\
\bar{Q}_{55} &= Q_{55}\cos^2\theta + Q_{44}\sin^2\theta.
\end{aligned} \tag{A.1}$$

Appendix B

1. The strains associated with the displacement field of CLPT are given by

$$\boldsymbol{\varepsilon} = \boldsymbol{\varepsilon}^{(0)} + z\boldsymbol{\varepsilon}^{(1)}, \tag{B.1}$$

$$\boldsymbol{\varepsilon}^{(0)} = \begin{Bmatrix} \varepsilon_{xx}^{(0)} \\ \varepsilon_{yy}^{(0)} \\ \varepsilon_{xy}^{(0)} \end{Bmatrix} = \begin{Bmatrix} \dfrac{\partial u_0}{\partial x} \\ \dfrac{\partial v_0}{\partial y} \\ \dfrac{\partial u_0}{\partial y} + \dfrac{\partial v_0}{\partial x} \end{Bmatrix}, \tag{B.2}$$

$$\boldsymbol{\varepsilon}^{(1)} = \begin{Bmatrix} \varepsilon_{xx}^{(1)} \\ \varepsilon_{yy}^{(1)} \\ \gamma_{xy}^{(1)} \end{Bmatrix} = \begin{Bmatrix} \dfrac{-\partial^2 w_0}{\partial x^2} \\ \dfrac{-\partial^2 w_0}{\partial y^2} \\ -2\dfrac{\partial^2 w_0}{\partial x \partial y} \end{Bmatrix}, \tag{B.3}$$

where $\boldsymbol{\varepsilon}^{(0)}$ and $\boldsymbol{\varepsilon}^{(1)}$ are the membrane and bending strains vectors, respectively.

2. The strains associated with the displacement field of FSDT are given by,

$$\boldsymbol{\varepsilon} = \boldsymbol{\varepsilon}^{(0)} + z\boldsymbol{\varepsilon}^{(1)}, \tag{B.4}$$

$$\boldsymbol{\gamma} = \boldsymbol{\gamma}^{(0)}, \tag{B.5}$$

$$\boldsymbol{\varepsilon}^{(0)} = \begin{Bmatrix} \varepsilon_{xx}^{(0)} \\ \varepsilon_{yy}^{(0)} \\ \gamma_{xy}^{(0)} \end{Bmatrix} = \begin{Bmatrix} \dfrac{\partial u_0}{\partial x} \\ \dfrac{\partial v_0}{\partial y} \\ \dfrac{\partial u_0}{\partial y} + \dfrac{\partial v_0}{\partial x} \end{Bmatrix}, \tag{B.6}$$

$$\boldsymbol{\varepsilon}^{(1)} = \begin{Bmatrix} \varepsilon_{xx}^{(1)} \\ \varepsilon_{yy}^{(1)} \\ \gamma_{xy}^{(1)} \end{Bmatrix} = \begin{Bmatrix} \dfrac{\partial \phi_x}{\partial x} \\ \dfrac{\partial \phi_y}{\partial y} \\ \dfrac{\partial \phi_x}{\partial y} + \dfrac{\partial \phi_y}{\partial x} \end{Bmatrix}, \tag{B.7}$$

$$\boldsymbol{\gamma}^{(0)} = \begin{Bmatrix} \gamma_{yz}^{(0)} \\ \gamma_{xz}^{(0)} \end{Bmatrix} = \begin{Bmatrix} \phi_y + \dfrac{\partial w_0}{\partial y} \\ \phi_x + \dfrac{\partial w_0}{\partial x} \end{Bmatrix}, \tag{B.8}$$

where $\boldsymbol{\varepsilon}^{(0)}$ and $\boldsymbol{\varepsilon}^{(1)}$ are the vectors of the membrane and bending strains, respectively, and $\gamma_{xy} = 2\varepsilon_{xy}$, $\gamma_{xz} = 2\varepsilon_{xz}$, $\gamma_{yz} = 2\varepsilon_{yz}$.

3. The strains associated with the displacement field of TSDT are given by

$$\boldsymbol{\varepsilon} = \boldsymbol{\varepsilon}^{(0)} + z\boldsymbol{\varepsilon}^{(1)} + z^3\boldsymbol{\varepsilon}^{(3)}, \tag{B.9}$$

$$\boldsymbol{\gamma} = \boldsymbol{\gamma}^{(0)} + z^2\boldsymbol{\gamma}^{(2)}, \tag{B.10}$$

$$\boldsymbol{\varepsilon}^{(0)} = \begin{Bmatrix} \varepsilon_{xx}^{(0)} \\ \varepsilon_{yy}^{(0)} \\ \gamma_{xy}^{(0)} \end{Bmatrix} = \begin{Bmatrix} \dfrac{\partial u_0}{\partial x} + \dfrac{1}{2}\dfrac{\partial^2 w_0}{\partial x^2} \\ \dfrac{\partial v_0}{\partial y} + \dfrac{1}{2}\dfrac{\partial^2 w_0}{\partial x^2} \\ \dfrac{\partial u_0}{\partial y} + \dfrac{\partial v_0}{\partial x} + \dfrac{\partial w_0}{\partial x}\dfrac{\partial w_0}{\partial y} \end{Bmatrix}, \tag{B.11}$$

$$\boldsymbol{\varepsilon}^{(1)} = \begin{Bmatrix} \varepsilon_{xx}^{(1)} \\ \varepsilon_{yy}^{(1)} \\ \gamma_{xy}^{(1)} \end{Bmatrix} = \begin{Bmatrix} \dfrac{\partial \phi_x}{\partial x} \\ \dfrac{\partial \phi_y}{\partial y} \\ \dfrac{\partial \phi_x}{\partial y} + \dfrac{\partial \phi_y}{\partial x} \end{Bmatrix}, \tag{B.12}$$

$$\boldsymbol{\varepsilon}^{(3)} = \begin{Bmatrix} \varepsilon_{xx}^{(3)} \\ \varepsilon_{yy}^{(3)} \\ \gamma_{xy}^{(3)} \end{Bmatrix} = -c_1 \begin{Bmatrix} \dfrac{\partial \phi_x}{\partial x} + \dfrac{\partial^2 w_0}{\partial x^2} \\ \dfrac{\partial \phi_y}{\partial y} + \dfrac{\partial^2 w_0}{\partial y^2} \\ \dfrac{\partial \phi_x}{\partial y} + \dfrac{\partial \phi_y}{\partial x} + 2\dfrac{\partial^2 w_0}{\partial x \partial y} \end{Bmatrix}, \tag{B.13}$$

$$\boldsymbol{\gamma}^{(0)} = \begin{Bmatrix} \gamma_{yz}^{(0)} \\ \gamma_{xz}^{(0)} \end{Bmatrix} = \begin{Bmatrix} \phi_y + \dfrac{\partial w_0}{\partial y} \\ \phi_x + \dfrac{\partial w_0}{\partial x} \end{Bmatrix}, \tag{B.14}$$

$$\boldsymbol{\gamma}^{(2)} = \begin{Bmatrix} \gamma_{yz}^{(2)} \\ \gamma_{xz}^{(2)} \end{Bmatrix} = -c_2 \begin{Bmatrix} \phi_y + \dfrac{\partial w_0}{\partial y} \\ \phi_x + \dfrac{\partial w_0}{\partial x} \end{Bmatrix}. \tag{B.15}$$

Here $c_2 = 3c_1$ and $\boldsymbol{\varepsilon}^{(0)}$, $\boldsymbol{\varepsilon}^{(1)}$ and $\boldsymbol{\varepsilon}^{(3)}$ are the vectors of the membrane, bending and warping strains, respectively.

Appendix C

The boundary conditions for a laminated plate simply supported on all edges are written as

$$\begin{aligned} u_0(x,0,t) &= 0, \quad w_0(0,y,t) = 0, \\ u_0(x,a,t) &= 0, \quad w_0(a,y,t) = 0, \\ v_0(0,y,t) &= 0, \quad w_0(x,0,t) = 0, \\ v_0(a,y,t) &= 0, \quad w_0(x,a,t) = 0, \end{aligned} \tag{C.1}$$

$$\begin{aligned} \frac{\partial w_0}{\partial x}(x,0,t) &= 0, \quad \frac{\partial w_0}{\partial y}(0,y,t) = 0, \\ \frac{\partial w_0}{\partial x}(x,a,t) &= 0, \quad \frac{\partial w_0}{\partial y}(a,y,t) = 0, \\ \phi_y(0,y,t) &= 0, \quad \phi_x(x,0,t) = 0, \\ \phi_y(a,y,t) &= 0, \quad \phi_x(x,a,t) = 0. \end{aligned} \tag{C.2}$$

To satisfy the boundary conditions, the displacements are expressed as follows

$$\begin{aligned} u_0(x,y,t) &= \sum_{n=1}^{\infty}\sum_{m=1}^{\infty} u_{mn}(t)\cos(\alpha x)\sin(\beta y), \\ v_0(x,y,t) &= \sum_{n=1}^{\infty}\sum_{m=1}^{\infty} v_{mn}(t)\sin(\alpha x)\cos(\beta y), \\ w_0(x,y,t) &= \sum_{n=1}^{\infty}\sum_{m=1}^{\infty} w_{mn}(t)\sin(\alpha x)\cos(\beta y), \\ \phi_x(x,y,t) &= \sum_{n=1}^{\infty}\sum_{m=1}^{\infty} X_{mn}(t)\cos(\alpha x)\sin(\beta y), \\ \phi_y(x,y,t) &= \sum_{n=1}^{\infty}\sum_{m=1}^{\infty} Y_{mn}(t)\sin(\alpha x)\cos(\beta y). \end{aligned} \tag{C.3}$$

Here $\alpha = \pi m/a$ and $\beta = \pi n/a$ where m and n are the half wavenumbers in the x and y directions, respectively, and $\mathbf{X}^{\mathrm{T}} = \{u_{mn}, v_{mn}, w_{mn}, X_{mn}, Y_{mn}\}$ is the unknown generalized displacement vector for the (m, n) mode.

References

[1] J.N. Reddy, *Mechanics of Laminated Composite Plates*, CRC press, Boca Raton, FL, 1997.

[2] A.K. Nayak, R.A. Shenoi, S.S.J. Moy, Analysis of damped composite sandwich plates using plate bending elements with substitute shear strain fields based on Reddy's higher-order-theory, *Proceedings of the Institution of Mechanical Engineering Part C—Journal of Mechanical Engineering Science* 216 (5) (2002) 591–606.

[3] H.Y. Kim, W. Huwang, Estimation of normal mode and other system parameter of composite laminated plates, *Composite Structures* 53 (2001) 345–354.

[4] D.A. Saravanos, D.A. Hopkins, Effects of délaminations on the damped dynamic characteristics of composites laminates: analysis and experiments, *Journal of Sound and Vibration* 192 (5) (1996) 977–993.

[5] M. Soula, T. Vinh, Y. Chevalier, T. Beda, T. Esteoule, Measurements of isothermal complex moduli of viscoelastic materials over a large range of frequencies, *Journal of Sound and Vibration* 205 (2) (1997) 167–184.

[6] J.H. Yim, J.W. Gillespie, Damping characteristics of 0° and 90° AS4/3501-6 unidirectional laminates including the transverse shear effect, *Journal of Composite Structures* 50 (2000) 217–225.

[7] M. Dalenbring, Experimental material damping estimation for planer isotropic laminate structures, *International Journal of Solid and Structures* 39 (2002) 5053–5079.

[8] A.Y.T. Leung, W.E. Zhou, Dynamic stiffness analysis of laminated composite plates, *Thin-Walled Structures* 25 (2) (1996) 109–133.

[9] Y. Ohta, Y. Narita, K. Nagasaky, On the damping analysis of FRP laminated composite plates, *Journal of Composite Structures* 57 (2002) 169–175.

[10] J.N. Reddy, T. Kuppusamy, Natural vibrations of laminated anisotropic plates, *Journal of Sound and Vibration* 94 (1) (1984) 63–69.

[11] K.H. Huang, A. Dasgupta, A layer-wise analysis for free vibration of thick composite cylindrical shells, *Journal of Sound and Vibration* 182 (2) (1995) 207–222.

[12] D.X. Lin, R.G. Ni, Adams, Prediction and measurement of the irrational damping parameters of carbon and glass fibre-reinforced plastics plates, *Journal Composite Material* 18 (1984) 132–152.

[13] N. Alam, N.T. Asnani, Vibration and damping analysis of fiber reinforced composite material plates, *Journal Composite Material* 20 (2) (1986) 2–18.

[14] J. Wang, K.M. Liew, M.J. Tan, S. Rajendran, Analysis of rectangular laminated composite plates via FSDT meshless method, *International Journal of Mechanical Sciences* 44 (2002) 1275–1293.

[15] C.W. Bert, T.L. Chen, Effect of shear deformation on vibration of antisymmetric angle-ply laminated rectangular plates, *International Journal of Solids and Structures* 14 (1978) 465–573.

[16] J.N. Reddy, Free vibration of antisymmetric angle-ply laminated plates including transverse shear deformation by the finite element method, *Journal of Sound and Vibration* 66 (1) (1979) 565–576.

[17] A.K. Noor, Free vibrations of multilayered composite plates, *American Institute of Aeronautics and Astronautics* 11 (7) (1973) 1038–1049.

[18] A. Khdeir, Free vibration and buckling of unsymmetric cross-ply laminated plates using a refined theory, *Journal of Sound and Vibration* 128 (3) (1989) 377–395.

[19] K.N. Koo, Vibration and damping analysis of composite plates using finite elements with layerwise in-plane displacements, *Computers and Structures* 80 (2002) 1393–1398.

[20] D. Zhou, Y.K. Cheung, J. Kongj, Free vibration of thick layered rectangular plates with point supports by finite layer method, *International Journal of Solids and Structures* 37 (2000) 1483–1499.

[21] M. Meunier, R.A. Shenoi, Dynamic analysis of composite sandwich plates with damping modelled using higher-order shear deformation theory, *Composite Structures* 54 (2001) 243–254.

[22] W. Ostachowicz, M. Krawczuk, A. Zak, Dynamics and buckling of a multilayer composite plate with embedded SMA wires, *Composite Structures* 48 (2000) 163–177.

[23] W. Hufenbach, C. Holste, L. Kroll, Vibration and damping behaviour of multi-layered composite cylindrical shells, *Composite Structures* 58 (2002) 165–174.

[24] G.L. Qian, S.V. Hoa, X. Xiao, A vibration method for measuring mechanical properties of composite theory and experiment, *Composite Structures* 39 (l–2) (1997) 31–38.

[25] S. Yarlagadda, G. Lesieutre, Fiber contribution to modal damping of polymer matrix composite panels, *Journal of Spacecraft and Rockets* 32 (5) (1995) 825–831.

[26] T. Pervez, N. Zabaras, Transient dynamic and damping analysis of laminated anisotropic plates using a refined plate theory, *International Journal for Numerical Methods in Engineering* 33 (5) (1992) 1059–1080.

[27] D.P. Makhecha, M. Canapathi, B.P. Patel, Vibration and damping analysis of laminated sandwich composite plates using higher order theory, *Journal of Reinforced Plastics and Composites* 216 (2002) 559–575.